Applied Physics Letters

Determining bandgap of black phosphorus using capacitance

Cite as: Appl. Phys. Lett. **116**, 183103 (2020); https://doi.org/10.1063/5.0010165
Submitted: 08 April 2020 . Accepted: 21 April 2020 . Published Online: 07 May 2020

Jialun Liu, Yujie Zhou, and Wenjuan Zhu

Hall Effect
Measurement Handbook
A comprehensive resource for researchers
Explore theory, methods, sources of errors,
and ways to minimize the effects of errors
Request it here
Lake Shore CRYOTRONICS

© 2020 Author(s).

Determining bandgap of black phosphorus using capacitance

Cite as: Appl. Phys. Lett. **116**, 183103 (2020); doi: 10.1063/5.0010165
Submitted: 8 April 2020 · Accepted: 21 April 2020 ·
Published Online: 7 May 2020

Jialun Liu, Yujie Zhou, and Wenjuan Zhu[a)]

AFFILIATIONS

University of Illinois at Urbana-Champaign, Urbana, Illinois 61801, USA

[a)]Author to whom correspondence should be addressed: wjzhu@illinois.edu

ABSTRACT

The bandgap of black phosphorus is widely tunable, depending on the number of layers, external electric field, and strain. Since the bandgap of black phosphorus is very narrow, it is difficult to measure using standard photoluminescence and absorption spectroscopy in the visible range. In this paper, we propose a method to extract the bandgap of black phosphorus using capacitance measured at various temperatures and frequencies. From the transition frequency or transition temperature, where C–V changes from high-frequency to low-frequency behavior, we can extract the bandgap information. Using this method, we extracted the bandgap of black phosphorus with a thickness of 50 nm to be 0.30 eV. For comparison, we also extracted the bandgap of black phosphorus using minimum conductance and threshold voltage methods, and the results are consistent with those of the C–V method. This C–V method can overcome the wavelength limitation of the photoluminescence measurement and spatial resolution limitation of Fourier transform infrared spectroscopy. Another advantage of this C–V method is that the extracted bandgap is unaffected by the contact resistance and device area, making it reliable and convenient in determining the bandgap of narrow bandgap materials.

Published under license by AIP Publishing. https://doi.org/10.1063/5.0010165

Black phosphorus (BP), a recent addition to the 2D family, brings new possibilities to nanoscale electronic and photonic devices. Black phosphorus has a puckered honeycomb structure, which yields unique anisotropic electrical, optical, and thermal properties.[1–5] The hole mobility of black phosphorus can reach 5200 cm^2/(V s) at room temperature and 45 000 cm^2/(V s) at 2 K, which makes it very promising for electronics.[6] Black phosphorus has a direct and tunable bandgap from 0.3 eV (bulk) to 1.4 eV (monolayer), corresponding to a broad energy spectrum from the infrared to visible frequency range, which opens up a wide range of applications in photonics.[3,7–11]

The bandgap of black phosphorus with a layer number larger than five is less than 0.7 eV based on the density function theory (DFT) calculation.[8,12] This narrow bandgap is beyond the wavelength range for most of the spectrometers in the photoluminescence (PL) measurements. In addition, the bandgap measured using PL is the optical gap, which is lower than the electronic bandgap due to the exciton binding energy. Recently, bandgap extractions based on current voltage (IV) measurements using a Schottky metal-oxide field-effect-transistor (MOSFET) model were demonstrated, which can measure the transport gap directly.[10,11] However, the accuracy of this method is highly dependent on the quality and the geometry of the devices, where the trap-assisted tunneling current and non-negligible resistance along the channel can cause errors in the extracted bandgap values. In this paper, we propose a C–V method to extract the bandgap of black phosphorus and compare it with the bandgap extracted using minimum conductance and threshold voltage methods.

Black phosphorus capacitors were fabricated on quartz substrates to eliminate the potential parasitic capacitance between the probe pads and substrates. The black phosphorus flakes were exfoliated from the bulk crystal and stacked onto the bottom metal electrodes using aligned dry transfer.[13] Hexagonal boron nitride (BN) was exfoliated from the bulk crystal and used as the dielectric in the capacitor. C–V measurements were performed in vacuum at frequencies ranging from 10 kHz to 4 MHz and at temperatures ranging from 6 K to 300 K. Ti/Au (5 nm/25 nm) was deposited to form source and drain contacts in BP transistors. The top gate dielectric is ∼30 nm HfO_2 deposited by atomic layer deposition (ALD).

The device structure of a black phosphorus capacitor is illustrated in Fig. 1(a). The BN thickness is ∼32 nm, and the black phosphorus thickness is ∼50 nm. The multi-frequency C–V curves of the BP/BN capacitor measured at 300 K are shown in Fig. 1(b). Here, the capacitance of the device, C, is normalized with respect to the gate dielectric capacitance, C_{ox}. At a measurement frequency of 63 kHz, C–V shows a typical low-frequency C–V behavior, where a local minimum is

Published under license by AIP Publishing

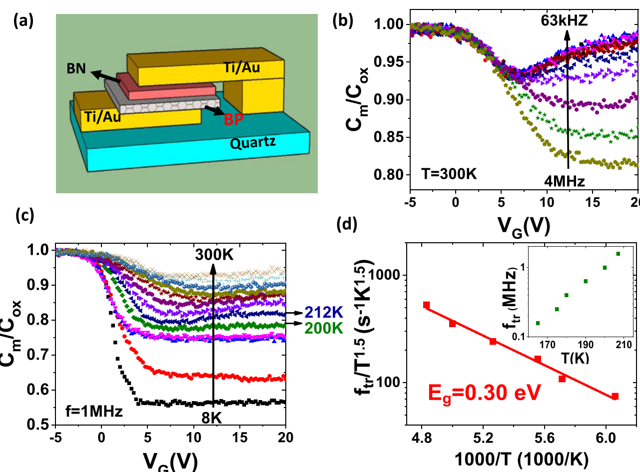

FIG. 1. Bandgap extracted using the C–V method. (a) Illustration of the BP/BN capacitors on the quartz substrate. (b) C–V curves of the BP/BN capacitor measured at 300 K with various frequencies. (c) C–V curves of the BP/BN capacitor measured at 1 MHz with various temperatures. (d) Transition frequency divided by $T^{1.5}$ as a function of 1000/T. The inset shows the transition frequency as a function of measurement temperature.

exhibited near the threshold voltage. As the frequency increases, the inversion capacitance decreases because the minority carriers in the inversion layer have more difficulty in following the fast AC signal. At 4 MHz, the semiconductor capacitance shows high-frequency C–V behavior, where the inversion capacitance remains at minimum capacitance even beyond threshold voltage.

This transition from high- to low-frequency behavior is also observed in the temperature dependence of the capacitances. Figure 1(c) shows the C–V curves for BP/BN capacitors measured at 1 MHz from 8 K to 300 K. We can see that there is large temperature dispersion in the inversion over this temperature range. At low temperature (8 K), the minority carriers could not follow the 1 MHz signal; thus, a high-frequency behavior is observed. However, as temperature increases, minority carriers begin to follow because the generation and recombination rates (G_{gr}) increase with temperature, so that the carrier response time ($\tau_R = C_D/G_{gr}$) decreases. Here, C_D is the depletion capacitance of the black phosphorus. As a result, the C–V curves change from high-frequency to low-frequency behavior as the temperature increases from 8 K to 300 K. Here, we define the transition frequency or transition temperature as the frequency or temperature where the C–V changes from a high-frequency to low-frequency behavior.[14] At a frequency of 1 MHz, the transition temperature is ~200 K for this BP capacitor, as shown in Fig. 1(c).

By measuring the C–V at various temperatures and frequencies, the temperature dependence of the transition frequency can be determined. The inset of Fig. 1(d) shows the transition frequency as a function of temperature. Assuming that the minority carrier response is dominated by the trap assistant process, the response time (τ_R) is inversely proportional to the intrinsic carrier density (n_i): $\tau_R \propto \frac{1}{n_i}$.[14] Here, the intrinsic carrier density can be expressed as $n_i = 2\left(\frac{2\pi kT}{h^2}\right)^{3/2}(m_n^* m_p^*)^{3/4} e^{-E_g/2kT}$, where m_n^* and m_p^* are the effective masses of electrons and holes, respectively, E_g is the bandgap, h is Planck's constant, k is Boltzmann's constant, and T is the temperature. The transition frequency can be expressed as $f_{tr} \approx 1/\tau_R$. From these equations, we can see that the transition frequency is

$$f_{tr} \propto T^{3/2} e^{-E_g/2kT}. \tag{1}$$

By plotting $\log(f_{tr}/T^{3/2})$ vs 1000/T, we can extract the bandgap from the slope, shown in Fig. 1(d). The extracted bandgap is ~0.30 eV for this BP flake, which is consistent with the DFT calculation and the bandgaps extracted from Schottky barriers.[8,11] Note that the bandgap extracted using the C–V method is independent of the doping concentration of black phosphorus and metal contact resistance. This feature provides an advantage of using C–V instead of I–V to extract the bandgap.

This transition frequency method provides a unique technique to extract the bandgap for narrow bandgap materials, such as black phosphorus. This C–V transition frequency technique can overcome the wavelength limit of the photoluminescence measurement and spatial resolution limit in Fourier transform infrared spectroscopy (FTIR). For indirect bandgap materials, since the photoluminescence signal is very weak, this electrical method to determine the bandgap will be very useful as well.

It has been reported previously that the bandgap of black phosphorus can be determined by minimum conductance. To compare the bandgaps extracted using these two methods, we fabricated BP transistors and measured the temperature dependence of the transfer characteristics. Since the thickness of the BP flakes is typically above 30 nm and the flakes are exfoliated from the same crystal, we expect that they will have similar bandgaps.[15] The transfer characteristics of the BP transistors are shown in Fig. 2(a). The motilities for holes and electrons are extracted from the linear regions of the transfer curves at the hole and electron branches, respectively. The hole and electron

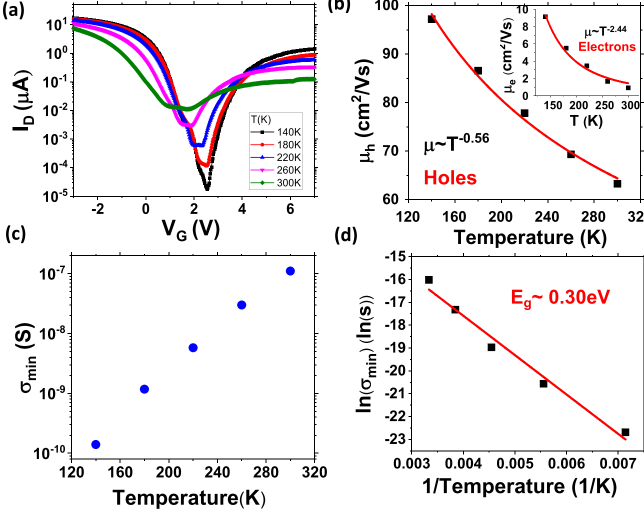

FIG. 2. Bandgap extracted using the minimum conductance method. (a) Ambipolar transfer characteristics of the BP transistor measured from 140 K to 300 K. (b) Effective hole mobility as a function of temperature. The inset shows the effective electron mobility as a function of temperature. (c) Minimum conductance as a function of temperature. (d) The bandgap of black phosphorus is extracted from the ln(σ_{min}) vs (1/T) plot.

Published under license by AIP Publishing

mobilities are plotted as a function of temperature, as shown in Fig. 2(b) and the inset of Fig. 2(b), respectively. By fitting the temperature dependence of the mobility using the equation $\mu \propto T^{-\Gamma}$,[16] we determine the Γ factor of this sample to be 0.56 for hole mobility and 2.44 for electron mobility. The minimum conductance as a function of temperature is shown in Fig. 2(c). The conductance (σ) can be expressed as $\sigma = q(n\mu_e + p\mu_h)$, where n and p are the carrier concentrations for electrons and holes and μ_e and μ_h are the mobilities for electrons and holes, respectively. When the conductance reaches the minimum, we have $\frac{\partial \sigma}{\partial p} = 0$. Considering $np = n_i^2$, we can derive the minimum conductance as follows:

$$\sigma_{\min} = 2qn_i\sqrt{\mu_e\mu_h}. \quad (2)$$

Since the intrinsic carrier concentration $n_i \propto T^{3/2}e^{-E_g/2kT}$ and $\sqrt{\mu_e\mu_h} \propto T^{-3/2}$ based on the Γ factors extracted in our sample, the minimum conductance follows $\sigma_{\min} \propto e^{-E_g/2kT}$. The BP bandgap could then be extracted from the plot of $\ln(\sigma_{\min})$ vs $(1/T)$, as shown in Fig. 2(d). The extracted bandgap of the BP flake is ∼0.30 eV, which is consistent with the results extracted from the C–V methods.

Another reported method to extract the bandgap using the IV measurement is based on the threshold voltages and subthreshold swing.[17–19] A transfer curve on the semi-log scale is drawn in Fig. 3(a), and the band diagrams at the threshold voltages for the electron and hole branches are illustrated in the insets of Fig. 3(a). When the Fermi level in the source electrode is lined up with the conduction band edge of the semiconductor channel, the gate voltage applied on the channel is defined as threshold voltage for the electron branch, V_{th-n}. When the Fermi level in the drain electrode is lined up with the valence band edge of the semiconductor channel, the gate voltage applied on the channel is defined as threshold voltage for the hole branch, V_{th-p} The subthreshold swing is $SS \equiv \ln(10)\frac{\partial V_G}{\partial \ln(I_D)} = \frac{kT}{q}\ln(10)\frac{\partial V_G}{\partial \psi_s} = SS_{ideal}\frac{\partial V_G}{\partial \psi_s}$, where ψ_s is the surface band bending in the semiconductor and $SS_{ideal} = \frac{kT}{q}\ln(10)$ is the thermodynamically limited subthreshold slope. Therefore, the bandgap of a semiconductor can be expressed as[17,18,20]

$$E_g = q\left[\frac{\Delta V_{th}}{(SS_p + SS_n)/2/SS_{ideal}}\right], \quad (3)$$

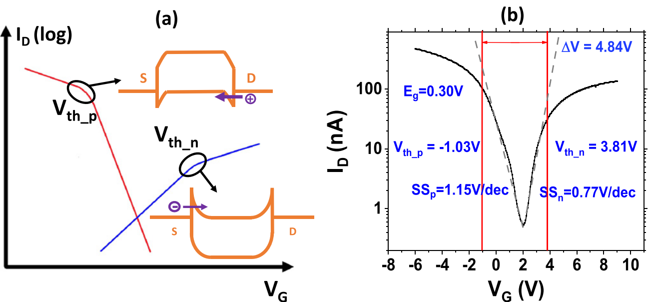

FIG. 3. Bandgap extraction based on the threshold voltage method. (a) Illustration of transfer characteristics of a Schottky-barrier transistor with a small bandgap semiconductor. The insets show the energy diagrams of the transistor at the threshold voltages for electron and hole branches. (b) I_D-V_G curve on the semi-log scale measured at 300 K with V_{DS} = 1 mV.

where q is the electron charge, $\Delta V_{th} = V_{th-n} - V_{th-p}$ is the difference between the threshold voltages for electron and hole branches, and SS_p and SS_n are the subthreshold swings in p and n branches, respectively. An example transfer curve measured at 300 K and the extracted threshold voltages are shown in Fig. 3(b). The bandgap extracted is 0.30 eV, which is consistent with that extracted using C–V and minimum conductance methods discussed previously.

Among these three methods of extracting the bandgap using electrical measurements, the C–V method uses the simplest device structure (two-terminal capacitor) and is least sensitive to the contact resistance. However, the C–V method is not practical for wide bandgap materials since the transition temperature in the standard frequency range (1 kHz ∼5 MHz) can reach >500 °C, which exceeds the temperature range for many probe stations. The threshold voltage method is the easiest and fastest method; however, its accuracy is undermined by the ambiguity in determining the threshold voltage in real devices' transfer curves. The minimum conductance method has moderate accuracy and complexity for narrow bandgap materials, but has very limited application in medium or wide bandgap materials, since the current at minimum conductance is below the detection level of the instrument if the bandgap is too large.

In summary, we proposed and demonstrated a method to determine the bandgap of black phosphorus using C–V measurements. Based on the transition frequency, at which the C–V characteristics change from high- to low-frequency behavior, we can extract the bandgap of the semiconductor. A 0.30 eV bandgap is determined for thick black phosphorus flakes (50 nm). For comparison, we also extracted the bandgaps using minimum conductance and threshold voltage methods. The bandgaps extracted from the three methods are consistent with each other. This method is especially useful for narrow and/or indirect bandgap materials, where photoluminescence measurements are beyond the spectrum range or detecting limit. The bandgap extracted using the C–V method is not affected by the contact resistance and device area, making it a convenient and accurate tool for characterizing the bandgaps of narrow bandgap materials.

AUTHORS' CONTRIBUTION

J.L. and Y. Z. contributed equally to this work.

This work was supported in part by the NSF under Grant Nos. ECCS 16–11279 and ECCS 16–53241 CAR and by ONR under Grant No. NAVY N00014–17-1–2973.

DATA AVAILABILITY

The data that support the findings of this study are available from the corresponding author upon reasonable request.

REFERENCES

[1]J. S. Qiao, X. H. Kong, Z. X. Hu, F. Yang, and W. Ji, "High-mobility transport anisotropy and linear dichroism in few-layer black phosphorus," Nat. Commun. **5**, 1–7 (2014).
[2]L. K. Li, Y. J. Yu, G. J. Ye, Q. Q. Ge, X. D. Ou, H. Wu, D. L. Feng, X. H. Chen, and Y. B. Zhang, "Black phosphorus field-effect transistors," Nat. Nanotechnol. **9**(5), 372–377 (2014).
[3]H. Liu, A. T. Neal, Z. Zhu, Z. Luo, X. F. Xu, D. Tomanek, and P. D. Ye, "Phosphorene: An unexplored 2D semiconductor with a high hole mobility," ACS Nano **8**(4), 4033–4041 (2014).

Published under license by AIP Publishing

[4] Z. Luo, J. Maassen, Y. X. Deng, Y. C. Du, R. P. Garrelts, M. S. Lundstrom, P. D. Ye, and X. F. Xu, "Anisotropic in-plane thermal conductivity observed in few-layer black phosphorus," Nat. Commun. **6**, 1–8 (2015).
[5] F. N. Xia, H. Wang, and Y. C. Jia, "Rediscovering black phosphorus as an anisotropic layered material for optoelectronics and electronics," Nat. Commun. **5**, 1–6 (2014).
[6] G. Long, D. Maryenko, J. Y. Shen, S. G. Xu, J. Q. Hou, Z. F. Wu, W. K. Wong, T. Y. Han, J. X. Z. Lin, Y. Cai, R. Lortz, and N. Wang, "Achieving ultrahigh carrier mobility in two-dimensional hole gas of black phosphorus," Nano Lett. **16**(12), 7768–7773 (2016).
[7] A. Castellanos-Gomez, L. Vicarelli, E. Prada, J. O. Island, K. L. Narasimha-Acharya, S. I. Blanter, D. J. Groenendijk, M. Buscema, G. A. Steele, J. V. Alvarez, H. W. Zandbergen, J. J. Palacios, and H. S. J. van der Zant, "Isolation and characterization of few-layer black phosphorus," 2D Mater. **1**(2), 025001–025019 (2014).
[8] V. Tran, R. Soklaski, Y. F. Liang, and L. Yang, "Layer-controlled band gap and anisotropic excitons in few-layer black phosphorus," Phys. Rev. B **89**(23), 1–6 (2014).
[9] X. M. Wang, A. M. Jones, K. L. Seyler, V. Tran, Y. C. Jia, H. Zhao, H. Wang, L. Yang, X. D. Xu, and F. N. Xia, "Highly anisotropic and robust excitons in monolayer black phosphorus," Nat. Nanotechnol. **10**(6), 517–521 (2015).
[10] S. Das, W. Zhang, M. Demarteau, A. Hoffmann, M. Dubey, and A. Roelofs, "Tunable transport gap in phosphorene," Nano Lett. **14**(10), 5733–5739 (2014).
[11] A. V. Penumatcha, R. B. Salazar, and J. Appenzeller, "Analysing black phosphorus transistors using an analytic Schottky barrier MOSFET model," Nat. Commun. **6**, 1–8 (2015).
[12] Y. Cai, G. Zhang, and Y. W. Zhang, "Layer-dependent band alignment and work function of few-layer phosphorene," Sci. Rep. **4**, 6677 (2015).
[13] A. Castellanos-Gomez, M. Buscema, R. Molenaar, V. Singh, L. Janssen, H. S. J. van der Zant, and G. A. Steele, "Deterministic transfer of two-dimensional materials by all-dry viscoelastic stamping," 2D Mater. **1**(1), 011002–011008 (2014).
[14] E. H. Nicollian and J. R. Brews, *MOS (Metal Oxide Semiconductor) Physics and Technology* (Wiley, New York, 1982).
[15] S. J. Liu, N. J. Huo, S. Gan, Y. Li, Z. M. Wei, B. J. Huang, J. Liu, J. B. Li, and H. D. Chen, "Thickness-dependent Raman spectra, transport properties and infrared photoresponse of few-layer black phosphorus," J. Mater. Chem. C **3**(42), 10974–10980 (2015).
[16] B. C. Deng, V. Tran, Y. J. Xie, H. Jiang, C. Li, Q. S. Guo, X. M. Wang, H. Tian, S. J. Koester, H. Wang, J. J. Cha, Q. F. Xia, L. Yang, and F. N. Xia, "Efficient electrical control of thin-film black phosphorus bandgap," Nat. Commun. **8**, 14474 (2017).
[17] S. Rosenblatt, Y. Yaish, J. Park, J. Gore, V. Sazonova, and P. L. McEuen, "High performance electrolyte gated carbon nanotube transistors," Nano Lett. **2**(8), 869–872 (2002).
[18] H. Tian, B. C. Deng, M. L. Chin, X. D. Yan, H. Jiang, S. J. Han, V. V. A. Sun, Q. F. Xia, M. Dubey, F. N. Xia, and H. Wang, "A dynamically reconfigurable ambipolar black phosphorus memory device," ACS Nano **10**(11), 10428–10435 (2016).
[19] H. L. Xu, S. Fathipour, E. W. Kinder, A. C. Seabaugh, and S. K. Fullerton-Shirey, "Reconfigurable ion gating of 2H-$MoTe_2$ field-effect transistors using poly(ethylene oxide)-$CsClO_4$ solid polymer electrolyte," ACS Nano **9**(5), 4900–4910 (2015).
[20] T. Chu, H. Ilatikhameneh, G. Klimeck, R. Rahman, and Z. H. Chen, "Electrically tunable bandgaps in bilayer MoS_2," Nano Lett. **15**(12), 8000–8007 (2015).

Published under license by AIP Publishing